

**EFFECT OF H₂SO₄/HClO₄ MIXTURE ON PROPERTIES OF SUGARCANE
BAGASSE CELLULOSE CRYSTALS**

NDUDUZO KHUMALO, SAMSON MOHOMANE
UNIVERSITY OF ZULULAND
SOUTH AFRICA

SETUMO V. MOTLOUNG^{1,2}

¹WALTER SISULU UNIVERSITY

²SEFAKO MAKGATHO HEALTH SCIENCE UNIVERSITY
SOUTH AFRICA

LEHLOHONOLO KOAO
UNIVERSITY OF THE FREE STATE (QWAQWA CAMPUS)
SOUTH AFRICA

MALEVU D. THEMBINKOSI
SEFAKO MAKGATHO HEALTH SCIENCE UNIVERSITY
SOUTH AFRICA

TSHWAFO E. MOTAUNG^{1,2}

¹SEFAKO MAKGATHO HEALTH SCIENCE UNIVERSITY

²UNIVERSITY OF SOUTH AFRICA
SOUTH AFRICA

RECEIVED (JUNE 2022)

ABSTRACT

The main objective of the study was to investigate the effect of mixed acid concentration on the morphology, crystallinity and thermal properties of cellulose nanocrystals (CNCs). Acid hydrolysis using mixture of sulphuric (H₂SO₄) acid and perchloric (HClO₄) acid was used to extract CNCs from sugarcane bagasse (SCB). The properties of the raw SCB, extracted cellulose, 45% H₂SO₄ hydrolysed CNCs, 45% H₂SO₄/HClO₄ hydrolysed CNCs, 55% H₂SO₄/HClO₄ hydrolysed CNCs and 65% H₂SO₄/HClO₄ hydrolysed CNCs were analysed using Fourier transmission infrared spectroscopy (FTIR), X-ray diffraction (XRD), scanning electron

microscopy (SEM) and thermogravimetric analysis (TGA). The crystallinity of SCB was significantly increased after bleaching and acid hydrolysis. Acid hydrolysis using 55% H₂SO₄/HClO₄ showed the highest crystallinity. The TGA results showed significant increase in thermal stability of 55% H₂SO₄/HClO₄. The lowest thermal stability was observed with 45% H₂SO₄ hydrolysed CNCs. The order of thermal stability was raw SCB < extracted cellulose < 45% H₂SO₄ hydrolysed CNCs < 65% H₂SO₄/HClO₄ hydrolysed CNCs < 45% H₂SO₄/HClO₄ hydrolysed CNCs < 55% H₂SO₄/HClO₄ hydrolysed CNCs. The SEM results showed fibre breakage for 65% H₂SO₄/HClO₄ hydrolysed CNCs. The fibre breakage seemed to be acid concentration dependent.

KEYWORDS: Sugarcane bagasse, cellulose, sulphuric acid, perchloric acid, nanocrystals.

INTRODUCTION

Recently, cellulose nanocrystals (CNCs) have attracted attention due to their significant abundance, renewability properties, low density and high reinforcing capabilities (Chen et al. 2019, Oun and Rhim 2016). Hence, they have also attracted significant applications in food packaging, cosmetics, polymers, biomedical amongst others (Hubbe et al. 2008, González et al. 2020, Ghafary et al. 2019, Abd Hamid et al. 2016, Akkera et al. 2017). Interestingly, the properties of CNCs are influenced by the choice of extraction method and the source of cellulosic material used (Oun and Rhim 2016). Furthermore, the isolation of CNCs is affected by reaction time, reaction temperature and the ratio of acid to fiber or cellulose (Arserim-Uçar et al. 2021). CNCs can be extracted through different methods including mechanical, enzymatic hydrolysis and acid hydrolysis treatment. However, acid hydrolysis is by far the widely used treatment of CNC isolation, particularly sulphuric acid (H₂SO₄) hydrolysis (Habibi et al. 2010, Peng et al. 2012). This might probably due stable suspension with high yield and crystallization produced, because of the sulphate ions (Zhong et al. 2020, Cui et al. 2016). On the contrary, CNCs isolated through H₂SO₄ hydrolysis produces suspensions with low thermal stability (Pandi et al. 2021, Ji et al. 2019). Therefore, many researchers have investigated acid hydrolysis using other acids such as HCl, H₃PO₄, HBr and HNO₃ (Yang et al. 2017, Pan et al. 2013, Kandhola et al. 2020). It has been discovered that CNCs extracted from these acids aggregate easily due to the abundance of surface hydroxyl groups which form strong intra- and inter-molecular hydrogen bonding interaction (Li et al. 2019, Zheng et al. 2019). In a study conducted by Correa et al. it was observed that the rate of fibre aggregation increased with the increase in HCl concentration (Corrêa et al. 2010). However, the resultant CNCs showed improved thermal properties when compare to H₂SO₄ hydrolysed CNCs. These two discoveries were due to the decrease in sulphate ions.

Therefore, the focus has shifted to the use of acid mixtures to isolate CNCs (Zhang et al. 2017, Kassab et al. 2020). The resultant CNCs typically showed excellent reinforcing properties in polymer nanocomposites manufacturing. Furthermore, they showed excellent dispersion in several organic solvents such as ethanol. The isolation of CNCs using HCOOH/HCl interestingly showed improved thermal and crystallinity properties due to the introduction of formate groups

in a study by Kassab et al. (2020). Moreover, it was apparent from the study that reinforcing and the reducibility are dependent on the capability formate group, thermal stability and crystallinity of CNCs. Maciel et. al. (2019) investigated the effect of acid hydrolysis conditions of 50 wt%, 60 wt% and 64 wt% of sulphuric acid. Among these three acid concentrations, the optimal properties were observed when using 64 wt% acid hydrolysis. However, in another study by Pan et. al. (2013), it was discovered that an increase in acid concentration from 20 to 60 wt% led to the breakage of CNCs fibres and produced suspension with lower crystallinity. It is apparent that the choice of acids used and the acid concentration have an effect in the properties of the resultant CNCs.

In this study, the effect of sulphuric acid mixed with perchloric acid (HClO_4) with varying acid concentration from 45 wt%, 55 wt% and 65 wt% was investigated. The thermal and morphological properties of $\text{H}_2\text{SO}_4/\text{HClO}_4$ hydrolysed CNCs extracted from sugarcane bagasse were determined.

MATERIALS AND METHODS

Materials

Sugarcane bagasse (SCB) waste was supplied by the sugar company at Empangeni (Felixton) in KwaZulu Natal, South Africa. Sodium hydroxide (NaOH) 99.9%, sodium hypochlorite (NaClO_2) 80%, glacial acetic acid (CH_3COOH), sulphuric acid (H_2SO_4) 95-99%, and perchloric acid (HClO_4) 60% were purchased at Merck Chemicals and used without being purified.

Extraction of cellulose

SCB was mechanically grounded using a Fritsch cutting mill pulveriser 15. The SCB was then boiled with distilled water for 2 hours and left in the oven to dry overnight at 55°C. The dried SCB was chemically treated with 4 wt% NaOH at 80°C for 1 hour followed by rinsing with distilled water. The process was repeated 2 times. The alkali treated SCB was then left in an oven to dry at 55°C overnight. The dried alkali treated SCB was then bleached using a buffer solution (54 g of NaOH and 150 ml of CH_3COOH mixed with 2L of 1.7 wt% solution of the NaClO_2 solution) for an hour at 80°C; this step was repeated 2 times. Finally, the bleached cellulose was filtered, washed with distilled water until a neutral pH was reached and dried overnight at 55°C.

Extraction of cellulose nanocrystals

The dried cellulose sample was finely crushed in a Fritsch cutting mill Pulveriser 15. A finely dried mass of 15 g of cellulose was weighed in 5 separate 600 ml beakers. A concentration of 45%, 55%, 65% $\text{H}_2\text{SO}_4/\text{HClO}_4$ mixture of acid and a 65% H_2SO_4 were prepared. A volume of 250 ml of 45% $\text{H}_2\text{SO}_4/\text{HClO}_4$ was added to a beaker in an ice bath of 10°C and stirred with a mechanical stirrer for 30 min. The reaction was then quenched with distilled water and left overnight. The mixture was then subjected to a centrifuge for 15 min. Subsequent, dialysis against distilled water was executed for 5 days until pH was neutral. Finally, the CNCs were then

dried in an oven over 5 days at 30°C. The same procedure was repeated for other acid concentrations.

Characterization methods

Fourier transform infra-red spectroscopy

Perkin Elmer attenuated total reflection FTIR spectrometer (Perkin Elmer UATR Two) operated in the diffuse reflectance mode was used to investigate structural functional groups of polymer samples. The spectral region between 4000 and 500 cm^{-1} was used during sample analysis.

X-ray diffraction

Bruker AXS Advance D8 diffractometer, Karlsruhe, Germany equipped with monochromatic Cu K α ($\lambda = 1.5406 \text{ \AA}$) as X-ray source operating at 40 kV and 40 mA at room temperature was used to investigate the crystallinity of all the materials studied. Both the Segal empirical method and deconvolution method were used to calculate the crystallinity index (CI) according to Park et al. (2010).

Scanning electron microscopy

FEI Quanta 200 electron microscopy operated at an accelerating voltage of 20 kV was used to investigate the morphological properties of the polymer materials studied. The samples were carbon-coated before analysis, using Edward's E306A coating system.

Thermogravimetric analysis

For the thermogravimetric analysis (TGA), the analysis was conducted using TGA analyser (Perkin Elmer Pyris 6). Samples ranging from 10-15 mg were heated at a temperature range 35 to 800°C at a heating rate of 5°C per min under nitrogen environment at a flow rate of 20 $\text{ml}\cdot\text{min}^{-1}$.

RESULTS AND DISCUSSION

FTIR spectroscopy analysis

The FTIR was employed to better understand the functional groups associated with CNCs after acid hydrolysis. The FTIR spectra of raw SCB, cellulose, $\text{H}_2\text{SO}_4/\text{HClO}_4$ hydrolysed CNCs (using 45%, 55% and 65% concentration of acid) and 45% H_2SO_4 hydrolysed CNCs are presented in Fig. 1.

The raw SCB showed characteristic of natural fibre with peaks observed at 3327 cm^{-1} (—OH stretching), 2896 cm^{-1} (C—H vibrations), 1361 cm^{-1} (—CH₂ bending), 1028 cm^{-1} (C—O stretching) and 892 cm^{-1} (—CH₂ bending) (Kalia et al. 2013, Wang et al. 2009, Ahmad et al. 2013, Hu et al. 2015, Lani et al. 2014, Kunaver et al. 2016). There was a noticeable addition of a peak at around 1309 cm^{-1} for all CNCs and extracted cellulose spectra which was absent for raw SCB. The peak maybe attributed to the C—H wagging when hydrogen bond was disrupted (Abidi et al. 2011). In addition, the extracted cellulose showed similar peaks patterns with the raw SCB, with

the addition of the peak around 1309 cm^{-1} . However, there was a decrease in peak intensity of peaks around 1434 and 1236 cm^{-1} and the increase in the peak intensity at 892 cm^{-1} which could be attributed to removal of the amorphous regions of cellulosic materials (Motaung et al. 2016, 2017).

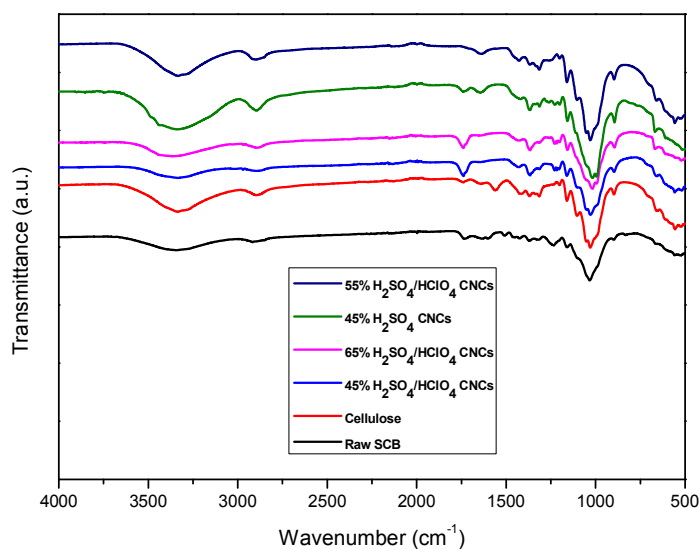


Fig. 1: FTIR spectra of the raw sugarcane bagasse, cellulose, 45% H_2SO_4 hydrolysed CNCs, 45% $\text{H}_2\text{SO}_4/\text{HClO}_4$ hydrolysed CNCs, 55% $\text{H}_2\text{SO}_4/\text{HClO}_4$ hydrolysed CNCs and 65% $\text{H}_2\text{SO}_4/\text{HClO}_4$ hydrolysed CNCs.

With regards to the 45% H_2SO_4 hydrolysed CNCs, the peaks appeared to be more pronounced with the absence of the peak at 1557 cm^{-1} when compared to the extracted cellulose which could be attributed to further removal of the amorphous regions of cellulosic materials (Motaung et al. 2016, 2017). For mixed acid hydrolysis, the 45% and 65% showed similar peak patterns with peaks around 3327 and 2896 cm^{-1} becoming more diminished compared to 55% acid concentrations. With the introduction perchloric acid, there was a removal of the peak around 1636 cm^{-1} attributed to the C=O stretching peak.

X-ray diffraction analysis

The XRD spectra of raw SCB, extracted cellulose, $\text{H}_2\text{SO}_4/\text{HClO}_4$ hydrolysed CNCs (using 45%, 55% and 65% concentration of acid) and 45% H_2SO_4 hydrolysed CNCs are shown in Fig. 2. The raw SCB material displayed peaks at $2\theta = 15, 23$ and 35° , typical of lignocellulosic material (Park et al. 2010). Moreover, the extracted cellulose showed similar behaviour compared to raw SCB with more pronounced peaks. Interestingly, the 45% H_2SO_4 hydrolysed CNCs and 65% $\text{H}_2\text{SO}_4/\text{HClO}_4$ hydrolysed CNCs displayed similar peaks at $2\theta = 12, 20, 22$ and 35° . However, the 55% $\text{H}_2\text{SO}_4/\text{HClO}_4$ hydrolysed CNCs displayed more pronounced peaks compared to 45% $\text{H}_2\text{SO}_4/\text{HClO}_4$ hydrolysed CNCs. In general, it can be noted that the intensity of the diffraction peak increased after chemical treatment for all the samples. These might be attributed by the removal of non-cellulosic materials such as hemicellulose, lignin and pectin.

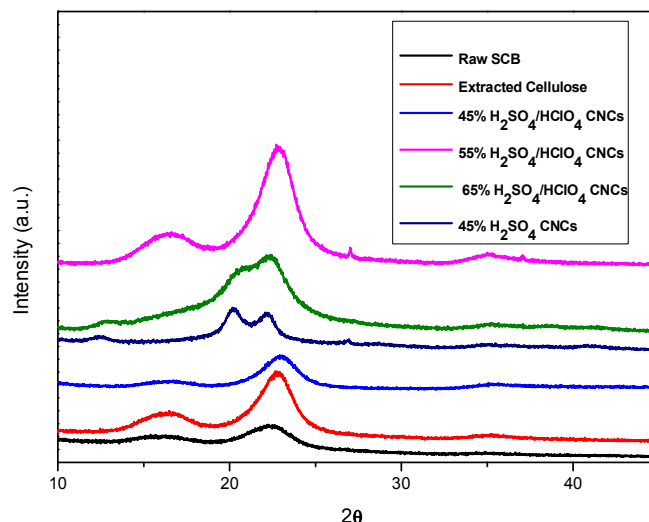


Fig. 2: XRD spectra of the raw sugarcane bagasse, cellulose, 45% H_2SO_4 hydrolysed CNCs, 45% $H_2SO_4/HClO_4$ hydrolysed CNCs, 55% $H_2SO_4/HClO_4$ hydrolysed CNCs and 65% $H_2SO_4/HClO_4$ hydrolysed CNCs.

Crystallinity index (CI) values were calculated using both the Segal empirical method and deconvolution methods as shown in Tab. 1. Generally, there was a notable increase in the values of CI values for extracted cellulose as compared to raw SCB. It is known that acid hydrolysis of native cellulose result in an increase in crystallinity index due to the removal lignin, hemicellulose and pectin after the chemical treatment (Motaung et al. 2017).

Tab. 1: Crystalline index values of materials studied using Segal and deconvolution methods.

Fiber type	CI (%) (Segal)	CI (%) (deconvolution)
Raw SCB	50	32
Cellulose	68	49
45% H_2SO_4 CNCs	72	51
45% $H_2SO_4/HClO_4$ CNCs	73	53
55% $H_2SO_4/HClO_4$ CNCs	76	56
65% $H_2SO_4/HClO_4$ CNCs	74	54

In addition, there was a further increase in CI after 45% H_2SO_4 hydrolysed CNCs which could be attributed to further removal of amorphous regions in CNCs. As for the mixed acid hydrolysis, 55% $H_2SO_4/HClO_4$ hydrolysed CNCs displayed the highest CI followed by 65% $H_2SO_4/HClO_4$ hydrolysed CNCs due to the high acidic concentration as well as the acidic strength of perchloric acid. Hence, the removal of the amorphous regions was easily achieved leading to formation of crystallites. The crystallinity index proved to be more favourable towards a 55% mixed acid. This may be due to the formation of strong enough acid to remove the amorphous regions and weak enough not to destroy the crystalline regions.

Scanning electron microscopy

SEM was conducted to investigate the morphological effect of mixed acid concentration on extracted CNCs. The SEM images of raw SCB, extracted cellulose, 45% H_2SO_4 hydrolysed

CNCs, 45% $H_2SO_4/HClO_4$ hydrolysed CNCs, 55% $H_2SO_4/HClO_4$ hydrolysed CNCs and 65% $H_2SO_4/HClO_4$ hydrolysed CNCs are presented in Fig. 3. In Fig. 3a, it can be clearly noticed that there are particles on the surface of the images. These particles are most probably due to the waxes, hemicellulose and pectin present in natural fibers. In addition, there were clearly absent from Fig. 3b as the bleaching removed these amorphous regions as confirmed by both FTIR and crystallinity results. It is also worth noting that extracted cellulose seems to have maintained its rod like structure compared to the rest CNCs which appeared a bit deformed (see arrows). Furthermore, it can be noted that the acid hydrolysis (Fig. 3c to 3e) did not result in any fibre breakage and pull-outs. These images showed smooth surface without fibre pull-outs and breakages. Fig. 3f showed characteristics of fibre breakage on the surface. This could be attributed to the high acid concentration. An acid concentration of 65% $H_2SO_4/HClO_4$ is strong enough to cause fibre breakages on the surface of CNCs. The results were further echoed by the crystallinity results. The decrease in CI observed from a 55% compared to a 65% meant the acid concentration is strong enough to cause fibre breakage hence decreasing CI (Abd Hamid et al. 2016).

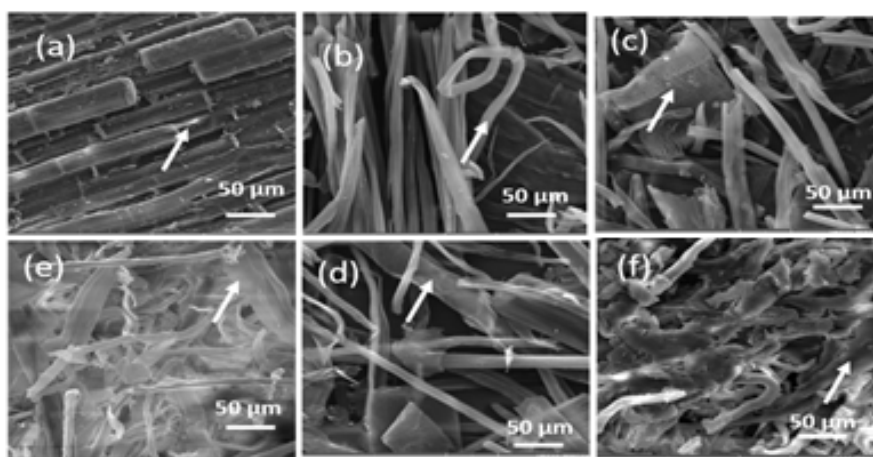


Fig. 3: SEM images of the (a) the raw sugarcane bagasse, (b) cellulose, (c) 45% H_2SO_4 hydrolysed CNCs, (d) 45% $H_2SO_4/HClO_4$ hydrolysed CNCs, (e) 55% $H_2SO_4/HClO_4$ hydrolysed CNCs and (f) 65% $H_2SO_4/HClO_4$ hydrolysed CNCs.

Thermogravimetric analysis

Thermogravimetric analysis studies were conducted to investigate the influence of acid concentration on the thermal properties of mixture of acids hydrolysed CNCs. The TGA and DTG curves are shown in Figs. 4 and 5 respectively. The raw SCB displayed two degradation steps with the high char content. The first degradation step around 333°C was attributed to removal of hemicellulose, waxes and pectin and the second degradation step at 492°C was attributed to lignin degradation (Arserim-Uçar et al. 2021, Mortari et al. 2014, Roman et al. 2004, Petrik et al. 2020). However, the extracted cellulose displayed one degradation step at around 337°C, which was attributed to non-cellulosic materials removal and gradual increase in thermal stability as compared raw SCB (Mortari et al. 2014). Furthermore, the 45% H_2SO_4 hydrolysed CNCs also displayed one degradation step at 342°C attributed to complete removal of amorphous regions by acid hydrolysis (Chen et al 2015). As for the mixture of acids

hydrolysed CNCs, the 45 and 65% acid concentration displayed similar degradation pattern as observed in the FTIR results with one degradation step at 347°C.

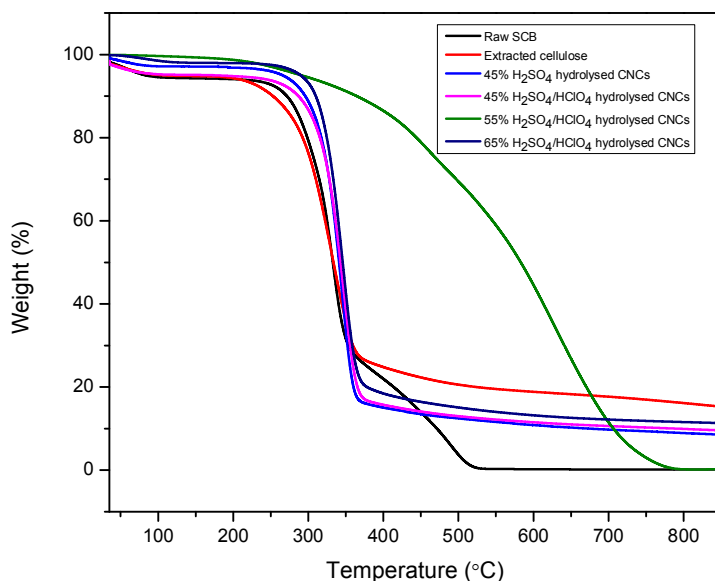


Fig. 4: TGA curve of the raw sugarcane bagasse, cellulose, 45% H₂SO₄ hydrolysed CNCs, 45% H₂SO₄/HClO₄ hydrolysed CNCs, 55% H₂SO₄/HClO₄ hydrolysed CNCs and 65% H₂SO₄/HClO₄ hydrolysed CNCs.

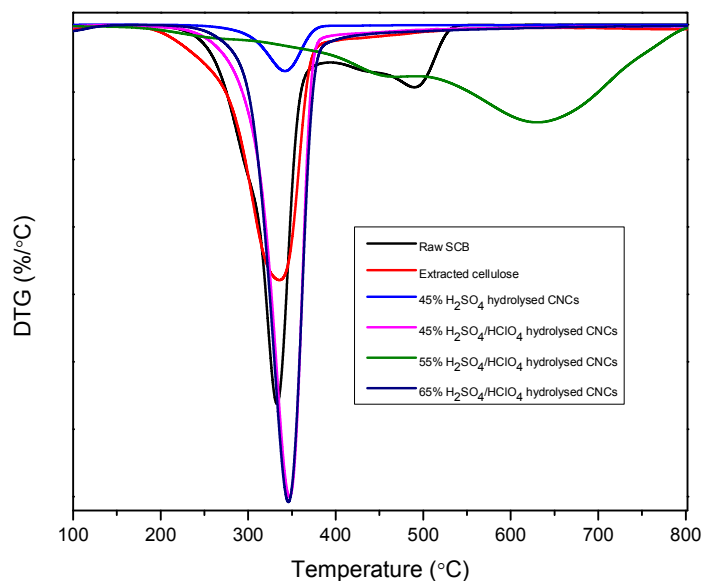


Fig. 5: DTG curve of the raw sugarcane bagasse, cellulose, 45% H₂SO₄ hydrolysed CNCs, 45% H₂SO₄/HClO₄ hydrolysed CNCs, 55% H₂SO₄/HClO₄ hydrolysed CNCs and 65% H₂SO₄/HClO₄ hydrolysed CNCs.

However, the 55% acid concentration displayed two degradation steps which are probably attributed to removal of oxygen atoms and the alteration of the furan rings in the condensed aromatic ring respectively. The thermal studies proved to be optimal for 55% H₂SO₄/HClO₄ hydrolysed CNCs as it was observed with the crystallinity results. The order of thermal stability was as follows: raw SCB < extracted cellulose < 45% H₂SO₄ hydrolysed CNCs < 65%

H₂SO₄/HClO₄ hydrolysed CNCs < 45% H₂SO₄/HClO₄ hydrolysed CNCs < 55% H₂SO₄/HClO₄ hydrolysed CNCs. The 45% H₂SO₄ hydrolysed CNCs displayed the lower thermal stability as compared to other mixture of acids hydrolysed CNCs (Pandi et al. 2021, Ji et al. 2019).

CONCLUSION

The main objective of the study was to investigate the effect of H₂SO₄/HClO₄ acid mixture concentration on crystallinity, morphological and thermal properties of the resultant CNCs. The XRD results showed an increase in crystallinity after the extraction of cellulose, with more pronounced results after mix acid hydrolysis. The increase in acid concentration from 45 wt% to 55 wt% resulted in increase in crystallinity index. The crystallinity results were echoed by both the SEM and the thermal studies. The SEM results showed broken fibres for 65 wt% acid concentrations which resulted in decrease in crystallinity index results. The results showed that acid hydrolysis using only H₂SO₄ resulted in lower thermal stability. Though, the addition of HClO₄ resultant in improved thermal stability of CNCs.

REFERENCES

1. Abd Hamid, S.B., Zain, S.K., Das, R., Centi, G., 2016: Synergic effect of tungstophosphoric acid and sonication for rapid synthesis of crystalline nanocellulose. *Carbohydrate Polymers* 138: 349-355.
2. Abidi, N., Hequet, E., Cabrales, L., 2011: Applications of Fourier transform infrared spectroscopy to study cotton fibers. Pp. 89-114, *Fourier Transforms - New Analytical Approaches and FTIR Strategies*. InTech.
3. Ahmad, E., Luyt, A., Djoković, V., 2013: Thermal and dynamic mechanical properties of bio-based poly (furfuryl alcohol)/sisal whiskers nanocomposites. *Polymer Bulletin* 70(4): 1265-1276.
4. Akkera, H.S., Reddy, N.N.K., Sekhar, M.C., 2017: Thickness dependent structural and electrical properties of magnetron sputtered nanostructured CrN thin films. *Materials Research* 20: 712-717.
5. Arserim-Uçar, D.K, Korel, F., Liu, L.S., Yam, K.L., 2021: Characterization of bacterial cellulose nanocrystals: Effect of acid treatments and neutralization. *Food Chemistry* 336: 127597.
6. Chen, Y., Liu, C., Chang, P.R., Cao, X., Anderson, D.P., 2009: Bionanocomposites based on pea starch and cellulose nanowhiskers hydrolyzed from pea hull fibre: effect of hydrolysis time. *Carbohydrate Polymers* 76(4): 607-615.
7. Chen, Z., Hu, M., Zhu, X., Guo, D., Liu, S., Hu, Z., Xiao, B., Wang, J., Laghari, M., 2015: Characteristics and kinetic study on pyrolysis of five lignocellulosic biomass via thermogravimetric analysis. *Bioresource Technology* 192: 441-450.
8. Corrêa, A., de Moraes Teixeira, E., Pessan, L., Mattoso, L.H.C.J.C., 2010: Cellulose nanofibers from curaua fibers. *Cellulose* 17: 1183-1192.

9. Cui, S., Zhang, S., Ge, S., Xiong, L., Sun, Q., 2016: Green preparation and characterization of size-controlled nanocrystalline cellulose via ultrasonic-assisted enzymatic hydrolysis. *Industrial Crops and Products* 83: 346-352.
10. Ghafary, S., Ranjbar, S., Larijani, B., Amini, M., Biglar, M., Mahdavi, M., Bakhshaei, M., Khoshneviszadeh, M., Sakhteman A., Khoshneviszade, M., 2019: Novel morpholine containing cinnamoyl amides as potent tyrosinase inhibitors. *International Journal of Biological Macromolecules* 135: 978-985.
11. González, M.M., Blanco-Tirado, C., Combariza, M.Y., 2020: Nanocellulose as an inhibitor of water-in-crude oil emulsion formation. *Fuel* 264: 116830.
12. Habibi, Y., Lucia, L.A., Rojas, O.J., 2010: Cellulose nanocrystals: chemistry, self-assembly, and applications. *Chemical Reviews* 110(6): 3479-3500.
13. Hu, F., Lin, N., Chang, P.R., Huang, J., 2015: Reinforcement and nucleation of acetylated cellulose nanocrystals in foamed polyester composites. *Carbohydrate Polymers* 129: 208-215.
14. Hubbe, M.A., Rojas, O.J., Lucia, L.A., Sain, M., 2008: Cellulosic nanocomposites: a review. *BioResources* 3(3): 929-980.
15. Ji, H., Xiang, Z., Qi, H., Han, T., Pranovich, A., Song, T., 2019: Strategy towards one-step preparation of carboxylic cellulose nanocrystals and nanofibrils with high yield, carboxylation and highly stable dispersibility using innocuous citric acid. *Green Chemistry* 21(8): 1956-1964.
16. Kalai, S., Thakur, K., Celli, A., Kiechel, M.A., Schauer, L.C., 2013: Surface modification of plant fibers using environment friendly methods for their application in polymer composites, textile industry and antimicrobial activities: A review. *Journal of Environmental Chemical Engineering* 1(3): 97-112.
17. Kandhola, G., Djiroleu, A., Rajan, K., Labbé, N., Sakon, J., Carrier, D.J., Kim, J.W., 2020: Maximizing production of cellulose nanocrystals and nanofibers from pre-extracted loblolly pine kraft pulp: a response surface approach. *Bioresources and Bioprocessing* 7(1): 1-16.
18. Kassab, Z., Kassem, I., Hannache, H., Bouhfid, R., Qaiss, A.E.K., Achaby, M.E., 2020: Tomato plant residue as new renewable source for cellulose production: extraction of cellulose nanocrystals with different surface functionalities. *Cellulose* 27(8): 4287-4303.
19. Kassab, Z., Tamraoui, Y., Hannache, H., Qaiss, A.E.K., Achaby, M.E., 2020: Characteristics of sulfated and carboxylated cellulose nanocrystals extracted from *Juncus* plant stems. *International Journal of Biological Macromolecules* 154: 1419-1425.
20. Kunaver, M., Anžlovar, A., Žagar, E., 2016: The fast and effective isolation of nanocellulose from selected cellulosic feedstocks. *Carbohydrate Polymers* 148: 251-258.
21. Lani, N.S., Ngadi, N., Johari, A., Jusoh, M., 2014: Isolation, characterization, and application of nanocellulose from oil palm empty fruit bunch fiber as nanocomposites. *Journal of Nanomaterials* 129: 208-215.
22. Li, H., Yan, Z., Xiong, Q., Chen, X., Lin, Y., Xu, Y., Bai, L., Jaing, W., Zheng, D., Xing, C., 2019: Renoprotective effect and mechanism of polysaccharide from *Polyporus umbellatus* sclerotia on renal fibrosis. *Carbohydrate Polymers* 212: 1-10.
23. Maciel, M.M.A.D., Benini, K.C.C.C., Voorwald, H.J.C., Cioffi, M.O.H., 2019: Obtainment and characterization of nanocellulose from an unwoven industrial textile cotton

- waste: Effect of acid hydrolysis conditions. *International Journal of Biological Macromolecules* 126: 496-506.
24. Mortari, D., Britto, M., Crnkovic, P., 2014: Correlation between activation energy and thermal decomposition yield of sugar cane bagasse under CO₂/O₂ and N₂/O₂. *Chemical Engineering Transactions* 37: 31-36.
 25. Motaung, T.E., Gqokoma, Z., Liganiso, L.Z., Hato, M.J., 2016: The effect of acid content on the poly (furfuryl) alcohol/cellulose composites. *Polymer Composites* 37(8): 2434-2441.
 26. Motaung, T.E., Liganiso, L.Z., Kumar, R., Anandijwala, R.D., 2017: Agave and sisal fibre-reinforced polyfurfuryl alcohol composites. *Journal of Thermoplastic Composite Materials* 30(10): 1323-1343.
 27. Oun, A.A., Rhim, J.W., 2016: Characterization of nanocelluloses isolated from Ushar (*Calotropis procera*) seed fiber: Effect of isolation method. *Materials Letters* 168: 146-150.
 28. Pan, M., Zhou, X., Chen, M., 2013: Cellulose nanowhiskers isolation and properties from acid hydrolysis combined with high pressure homogenization. *BioResources* 8(1): 933-943.
 29. Pandi, N., Sonawane, S.H., Kishore, K.A., 2021: Synthesis of cellulose nanocrystals (CNCs) from cotton using ultrasound-assisted acid hydrolysis. *Ultrasonics Sonochemistry* 70: 105353.
 30. Park, S., Baker, J.O., Himmel, M.E., Parilla, P.A., Johnson, D.K., 2010: Cellulose crystallinity index: measurement techniques and their impact on interpreting cellulase performance. *Biotechnology for Biofuels* 3(1): 1-10.
 31. Peng, Y., Gardner, D.J., Han, Y., 2012: Drying cellulose nanofibrils: in search of a suitable method. *Cellulose* 19(1): 91-102.
 32. Petrik, L.F., Abiaziem, C., Williams, A.B., 2020: Isolation and characterisation of cellulose nanocrystal obtained from sugarcane peel. *Rasayan Journal Chemistry* 13(1): 177-187.
 33. Roman, M., Winter, W.T., 2004: Effect of sulfate groups from sulfuric acid hydrolysis on the thermal degradation behavior of bacterial cellulose. *Biomacromolecules* 5(5): 1671-1677.
 34. Wang, L., Kumar, R., Zhang, L., 2009: Investigation into hemp fiber-and whisker-reinforced soy protein composites. *Frontiers of Chemistry in China* 4(3): 313-320.
 35. Yang, X., Han, F., Xu, C., Jiang, S., Huang, L., Liu, L., Xia, Z., 2017: Effects of preparation methods on the morphology and properties of nanocellulose (NC) extracted from corn husk. *Industrial Crops and Products* 109: 241-247.
 36. Zhang, H., Yu, H.Y., Wang, C., Yao, J., 2017: Effect of silver contents in cellulose nanocrystal/silver nanohybrids on PHBV crystallization and property improvements. *Carbohydrate Polymers* 173: 7-16.
 37. Zheng, D., Zhang, Y., Guo, Y., Yue, J., 2019: Isolation and characterization of nanocellulose with a novel shape from walnut (*Juglans regia* L.) shell agricultural waste. *Polymers* 11(7): 1130.
 38. Zhong, T., Dhandapani, R., Liang, D., Wang, J., Wolcott, M.P., Fossen, D.V., Liu, H., 2020: Nanocellulose from recycled indigo-dyed denim fabric and its application in composite films. *Carbohydrate Polymers* 240: 116283.

NDUDUZO KHUMALO, SAMSON MOHOMANE
UNIVERSITY OF ZULULAND
KWADLANGEZWA CAMPUS
DEPARTMENT OF CHEMISTRY
PRIVATE BAG X1001, KWADLANGEZWA 3886
KWAZULU NATAL, SOUTH AFRICA

SETUMO V. MOTLOUNG^{1,2}

¹WALTER SISULU UNIVERSITY
DEPARTMENT OF CHEMICAL AND PHYSICAL SCIENCES
PRIVATE BAG X1, MTHATHA CAMPUS, UNITRA 5117
SOUTH AFRICA

²SEFAKO MAKGATHO HEALTH SCIENCES UNIVERSITY
DEPARTMENT OF PHYSICS
P.O. BOX 94, MEDUNSA 0204, SOUTH AFRICA

LEHLOHONOLO KOAO
UNIVERSITY OF THE FREE STATE (QWAQWA CAMPUS)
DEPARTMENT OF PHYSICS
PRIVATE BAG X13, PHUTHADITJHABA 9866, SOUTH AFRICA

MALEVU D. THEMBINKOSI
SEFAKO MAKGATHO HEALTH SCIENCES UNIVERSITY
DEPARTMENT OF PHYSICS
P.O. BOX 94, MEDUNSA 0204, SOUTH AFRICA

TSHWAFO E. MOTAUNG*^{1,2}

¹SEFAKO MAKGATHO HEALTH SCIENCES UNIVERSITY
DEPARTMENT OF CHEMISTRY
P.O. BOX 94, MEDUNSA 0204, SOUTH AFRICA

²UNIVERSITY OF SOUTH AFRICA
DEPARTMENT OF CHEMISTRY
SCHOOL OF SCIENCE IN THE COLLEGE OF SCIENCE ENGINEERING AND
TECHNOLOGY
PRELLER STREET, MUCKLENEUK RIDGE, CITY OF TSHWANE
P.O. BOX 392, UNISA 0003, SOUTH AFRICA

*Corresponding author: motaungte@live.com or motaute1@unisa.ac.za